

Trigonometric parallax measurements of post-AGB stars with VERA

Hiroshi Imai¹, Daniel Tafoya¹, and VERA collaboration^{1,2}

¹Department of Physics and Astronomy, Graduate School of Science and Engineering, Kagoshima University, 1-21-35 Korimoto, Kagoshima 890-0065, Japan
 email: hiroimai@sci.kagoshima-u.ac.jp

²Mizusawa VLBI Observatory, National Astronomical Observatory of Japan, 2-21-1 Osawa, Mitaka, Tokyo 181-8588, Japan

Abstract. A trigonometric parallax distance is measurable for a planetary nebula if it harbors H₂O (or OH) maser spots. We have demonstrated it for H₂O maser sources, K3–35, IRAS 19312+1950 and IRAS 18286–0959 using the VLBI Exploration of Radio Astrometry (VERA). They are post-AGB stars and exhibit peculiar morpho-kinematical structures like a bipolar planetary nebula or a bipolar molecular jet (water fountain). The luminosities and secular motions of these sources derived from the trigonometric distances and proper motions of the H₂O masers suggest that their parental stars may be intermediate-mass ($2M_{\odot} < M_{*} < 8M_{\odot}$) evolved stars.

Keywords. masers, stars:distances, individuals (K3–35, IRAS 19312+1950, IRAS 18286–0959)

Dual-beam receiving system equipped in the VERA telescopes enables us to simultaneously track a Galactic H₂O maser source and an position-reference quasar, yielding sub-milliarcsecond-level astrometry between the two sources separated by 0.3°–2.0°. In spite of high time variability of the H₂O masers, a few maser spots survive for one year or longer, enabling us to monitor their motions to measure their trigonometric parallaxes and linear proper motions.

We have conducted astrometric VLBI observations of H₂O masers in three post-AGB stars with VERA. Fig. 1, 2) show some results of the astrometry. Table 1 gives astrometric and Galactic kinematical parameters of these sources obtained from the astrometry. These sources harbor bipolar morphology of PNe or “water fountains” (WFs). From the VERA astrometry, we have learnt the following issues.

1. Stellar luminosities derived from the spectral energy distributions and the trigonometric parallax distances are higher than 10000 L_{\odot} (for IRAS 18286–0959, IRAS 19312+1950).
2. Large deviations from the Galactic circular rotation ($>50 \text{ km s}^{-1}$ for IRAS 18286–0959) implies the kinematical property different from that of massive young stellar objects in the Galactic thin disk. These implies that the central stars may be intermediate-mass post AGB stars. Our recent sub-mm CO line observations also support this mass estimation (Imai *et al.* in preparation).

Table 1. Source parameters derived from the VERA astrometry.

| Object | Type | D (kpc) | R_{Gal}^{\dagger} (kpc) | z^{\ddagger} (pc) | V_R^* (km s^{-1}) | V_{θ}^* (km s^{-1}) | V_z^* (km s^{-1}) | Reference |
|-----------------|--------|---------------------|-------------------------------------|------------------------|-----------------------------------|--|-----------------------------------|-----------------------------|
| K3–35 | PN | $3.9^{+0.7}_{-0.5}$ | $7.11^{+0.08}_{-0.06}$ | 140^{+25}_{-18} | 33 ± 16 | 233 ± 11 | 11 ± 2 | Tafoya <i>et al.</i> (2011) |
| IRAS 19312+1950 | Pre-PN | $3.8^{+0.8}_{-0.6}$ | 7.07 ± 0.12 | 28 ± 3 | 33 ± 28 | 214 ± 4 | -14 ± 8 | Imai <i>et al.</i> (2011) |
| IRAS 18286–0959 | WF | $3.9^{+1.1}_{-0.7}$ | 4.93 ± 0.69 | 22 ± 2 | 64 ± 30 | 133 ± 36 | -17 ± 31 | Imai <i>et al.</i> in prep. |

[†]Galactocentric distance to the object.

[‡]Height from the Galactic midplane.

* V_R , V_{θ} , and V_z are the secular motion vector components in the Galactic radial, azimuthal, and rotation axis directions, respectively.

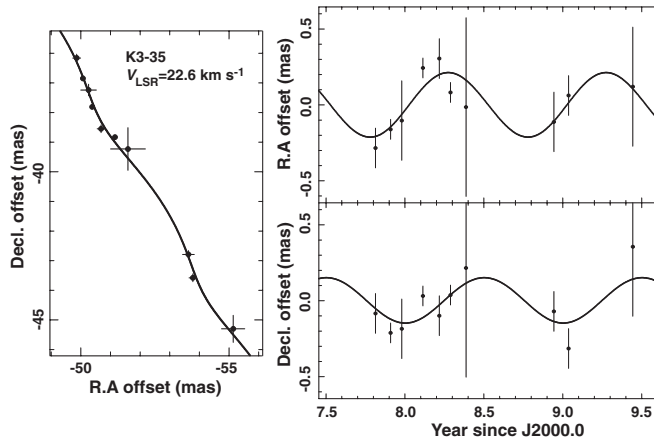


Figure 1. H_2O maser spot position in K3–35 (filled circle) and the kinematical model for the spot's motion. *Left* R.A. and decl. offsets. solid curve shows the modeled motion including an annual parallax and a constant velocity proper motion. *Right* R.A. and decl. variations of the spot position along time. The estimated annual parallax and linear proper motion are subtracted from the observed spot position.

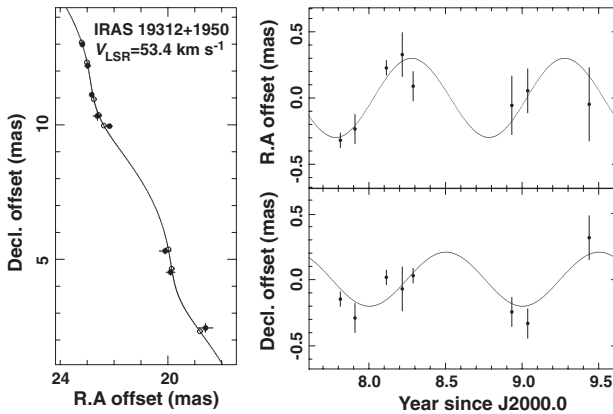


Figure 2. Same as Fig. 1 but for IRAS 19312+1950 (Imai *et al.* 2011).

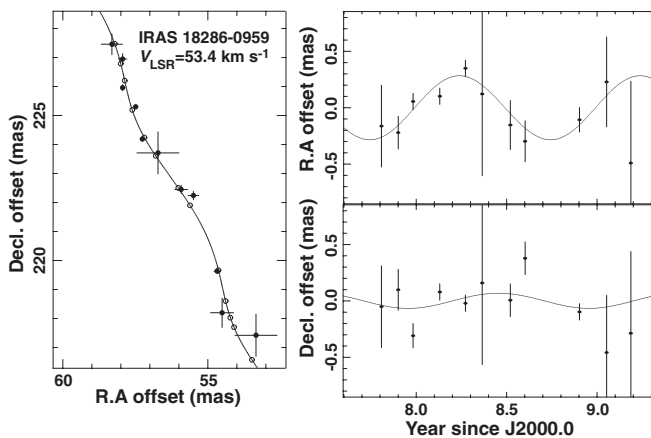


Figure 3. Same as Fig. 1 but for IRAS 18286–0959 (Imai *et al.* in preparation.)

References

- Imai, H., Tafoya, D., Honma, M., Hirota, T., Miyaji, T. 2011, *PASJ*, 63, 87
 Tafoya, D., *et al.* 2011, *PASJ*, 63, 71